Design of a Scaled-down DRACS Test Facility for an AHTR

X. Wang[1], Q. Lv[1], X. Sun[1], R.N. Christensen[1], T.E. Blue[1], G. Yoder[2], D. Wilson[2], and P. Sabharwall[3]

[1]: *Nuclear Engineering Program, The Ohio State University*
201 West 19th Avenue, Columbus, OH 43210
wang.1037@osu.edu, lv.11@buckeyemail.osu.edu, sun.200@osu.edu, christensen.3@osu.edu and blue.1@osu.edu
[2]: *Oak Ridge National Laboratory, Oak Ridge, TN 37380,* yodergljr@ornl.gov *and* wilsondf@ornl.gov
[3]: *Idaho National Laboratory, Idaho Falls, ID 83402,* Piyush.Sabharwall@inl.gov

INTRODUCTION

A Direct Reactor Auxiliary Cooling System (DRACS) has been proposed for an Advanced-High Temperature Reactor (AHTR) that uses fluoride salt as the coolant. A study is being carried out to test its performance and provide experimental data for model validation. A detailed scaling analysis has been performed for the DRACS, as reported in a companion paper [1], in which a scaling methodology is developed. In this paper, the scaling results for a prototypic DRACS design are presented to design a scaled-down DRACS test facility.

CORE SCALING ANALYSIS

As discussed in Ref. [1], the scaling process with the convection time ratio in the primary loop was considered, which is related to the convective heat transfer coefficient and structure properties of the reactor core.

The heat transfer in a pebble bed core could be dominated by the natural, forced, or mixed convection, depending on the flow's Reynolds number and Grashof number, which are respectively defined as:

$$\mathrm{Re} \equiv \frac{D_p G}{\mu}, \tag{1}$$

$$\mathrm{Gr} \equiv \frac{g\beta \Delta T D_p^3}{\nu^2}. \tag{2}$$

Here, D_p, g, G, β, ΔT, μ, and ν are the pebble diameter, gravitational acceleration, mass flux, thermal expansion coefficient, temperature difference, dynamic viscosity, and kinematic viscosity of the fluid, respectively. The Reynolds number in the core is estimated as 3.9 when 1% decay power is assumed for a 20-MWth prototypic AHTR. This is far below the application ranges of most heat transfer correlations available for a pebble bed configuration in the literature. In view of this, the mass transfer correlations for low Reynolds numbers proposed by Karabales et al. [2] are adopted by analogizing the Sherwood number to the Nusselt number and the Schmidt number to the Prandtl number. The Nusselt number for different flow regimes were given as [2]:

Mixed laminar convection:

$$\mathrm{Nu} = \left[\left\{0.46\left(\mathrm{Gr}\,\mathrm{Pr}\right)^{1/4}\right\}^6 + \left\{4.58\,\mathrm{Re}^{1/3}\,\mathrm{Pr}^{1/3}\right\}^6\right]^{1/6}, \tag{3}$$

Mixed turbulent convection:

$$\mathrm{Nu} = \left[\left\{0.112\left(\mathrm{Gr}\,\mathrm{Pr}\right)^{1/3}\right\}^2 + \left\{2.39\,\mathrm{Re}^{0.56}\,\mathrm{Pr}^{1/3}\right\}^2\right]^{1/2}; \tag{4}$$

Forced convection:

$$\mathrm{Nu} = \left[\left\{4.58\,\mathrm{Re}^{1/3}\,\mathrm{Pr}^{1/3}\right\}^6 + \left\{2.39\,\mathrm{Re}^{0.56}\,\mathrm{Pr}^{1/3}\right\}^6\right]^{1/6}. \tag{5}$$

The relations between the Reynolds number and Grashof number when the flow transitions from the mixed to forced convection are obtained, as shown in Fig.1. In the present case, the Reynolds number and Grashof number are 3.9 and 4.6×10^5, respectively, leading to a mixed laminar condition. The Nusselt number is 22.1 based on Eq. (3), and the convective heat transfer coefficient is 832 W/m^2-K when FLiBe (^{7}LiF-BeF$_2$, with 67-33 in mol%) is used as the primary coolant.

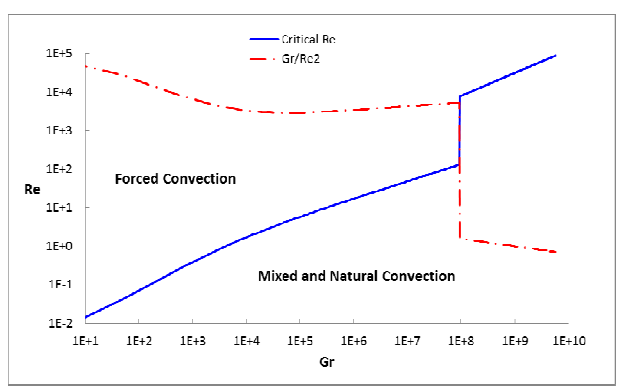

Fig. 1. Relations between the critical Reynolds number and Grashof number for flow transitions from the mixed to forced convection

In a prototypic AHTR design, spherical fuel pebbles with 30 mm diameter shown in Fig. 2 are employed [3]. TRISO particles are embedded within a spherical shell in the pebbles with high-density graphite as the binder. This spherical shell surrounds a low-density graphite sphere in the center of the pebble that affects the overall density of the TRISO particle. The detailed information on the dimensions of the pebbles and TRISO particle is listed in Table 1.

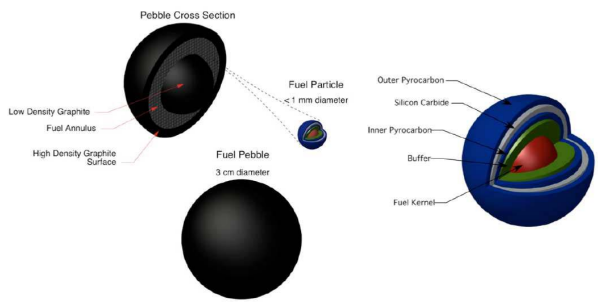

Fig. 2. Structure of a fuel pebble and TRISO particle [3]

Table 1 Dimensions of the spherical fuel pebble and TRISO particle [4]

Spherical fuel pebble					
Graphite kernel radius (mm)	Fuel zone outer radius (mm)	Coating thickness (mm)	Total # of TRISO	Volumetric fraction of TRISO	
9.92	12.5	2.5	2,144	20%	
TRISO particle					
Layer	Fuel kernel	Porous carbon	Pyro-carbon	SiC	Pyro-carbon
Radius (mm)	0.251	0.3425	0.3824	0.4177	0.4577

The effective properties of the entire pebble were evaluated based on the properties of the materials composing the fuel pebbles. For the high-density coating and filling graphite in the fuel pebbles, H-451 that is used as the structural graphite in HTGRs was adopted. The information on material properties was summarized by Gougar et al. [5]. The physical properties of these materials depend on their temperature and per Ref. [4], were evaluated in this study based on a reference temperature of 750 ^{o}C. In addition, the thermal conductivity is also a function of the received neutron fluence.

We used volumetric averaging to evaluate the effective density and mass weighted averaging to evaluate the effective specific heat capacity. The determination of the effective thermal conductivity was rather complicated and consisted of three steps. First, we considered that the total thermal resistance of a TRISO particle is in series and computed by the summation of individual thermal resistance. The harmonic average was therefore used to obtain the effective thermal conductivity of the TRISO particle (k_{TRI}) as follows:

$$k_{TRI} = \frac{V}{\sum V_i / k_i}, \tag{6}$$

where i is the layer index inside the TRISO particle. Secondly, we treated the spherical shell, in which the TRISO particles are embedded in H-451 filling as a porous medium. We applied Maxwell-Eucken-I model [6] to calculate the effective thermal conductivity of this spherical shell (k_{ann}) as:

$$k_{ann} = \frac{k_{H451}V_{H451} + k_{TRI}V_{TRI}[3k_{H451} / (2k_{H451} + k_{TRI})]}{V_{H451} + V_{TRI}[3k_{H451} / (2k_{H451} + k_{TRI})]}. \tag{7}$$

Thirdly, Eq. (6) was used to calculate the effective thermal conductivity of the entire pebble. The calculated values of the effective properties of a pebble are given in Table 2.

Table 2 Effective properties of a fuel pebble

Fluence ($\times 10^{25}$ n/m^2)	0	0.1	0.2	0.5	1	3-8
k (W/m-K)	65.89	55.6	47.16	30.77	22.31	20.4
c_p (J/kg-K)	1,635					
ρ (kg/m^3)	1,894					

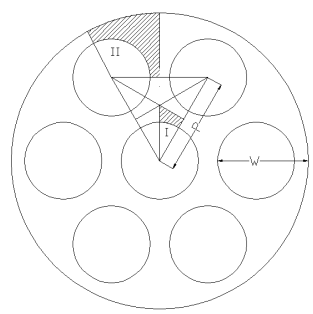

Fig. 3. Core design in experiment

Next, a heater bundle as shown in Fig. 3 was chosen to emulate the reactor core in our experiments. It consists of 7 electric heater rods arranged in an equilateral triangular pattern in a circular vessel. The flow channels are categorized into the interior sub-channel (type I), and the wall sub-channel (type II). Heat transfer coefficients in such an arrangement were obtained by Mohanty and Sahoo [7, 8]. We adopted the design with P/D of 1.6 and W/D of 1.4 since this configuration results in a large Nusselt number for the wall sub-channel. Here, P, W, and D are the pitch, shell wall spacing, and rod diameter,

respectively. The effective Nusselt number was calculated by area-weighted averaging. The relevant information is summarized in Table 3.

Table 3 Design parameters of heater rods

	30° interior sub-channel (type I)	120° wall sub-channel (type II)	Average
#	36	12	
D (mm)	9.5	9.5	
P/D	1.6	1.6	
W/D	--	1.4	
D_h (mm)	17	13	14
Nu	12.18	5.742	8.44

Furthermore, FLiNaK (LiF-NaF-KF, with 46.5-11.5-42 in mol%) was chosen as both the primary and secondary coolants in our experiment, due to its low price, low toxicity, and high thermal conductivity. With this salt, the average heat transfer coefficient considering the interior and wall sub-channels in the simulated core in our typical experiment was estimated as 511 W/m^2-K. Incoloy 800H was adopted as the heater sheath material.

SUMMARY OF SCALING ANALYSIS

Table 4 Loop scaling results

Fluence ($\times 10^{25}$ n/m^2)		0	**0.1**	0.2	0.5	1	3-8
Power (kW)		**8.48**					
Power ratio		**4.24%**					
Primary loop							
Time ratio		1.11	**1.31**	1.55	2.37	3.27	3.57
Length ratio		0.5	**0.5**	0.5	0.5	0.5	0.5
D_h ratio in Core	From scaling	0.84	**0.99**	1.17	1.80	2.48	2.71
	From design	1.07					
δ ratio in core		0.58	**0.68**	0.80	1.23	1.70	1.86
Velocity ratio		0.45	**0.38**	0.32	0.21	0.15	0.14
Area ratio		0.08	**0.14**	0.22	0.80	2.10	2.75
ΔT ratio		0.28	**0.20**	0.15	0.06	0.03	0.03
Heat source number ratio		155	**258**	422	1521	3991	5220
Secondary loop							
Time ratio		1.11	**1.31**	1.55	2.37	3.27	3.57
Length ratio		1	**1**	1	1	1	1
Velocity ratio		0.90	**0.76**	0.65	0.42	0.31	0.28
Area ratio		0.01	**0.02**	0.03	0.11	0.30	0.39
ΔT ratio		0.82	**0.58**	0.42	0.18	0.09	0.08

With all the necessary information, the convection time ratio was obtained and the complete scaling analysis of the DRACS was accomplished. The analysis of the heat exchangers, i.e., DHX and NDHX, was performed with Incoloy 800H as the structure and piping materials. In addition, the same power ratio and convection time ratio were assumed for both the primary and secondary loops of the DRACS. The results are summarized in Tables 4 and 5, in which the column in bold gives the best scaling results. This is the case when the reactor has been operated for about 160 days with an average neutron flux level of 10^{13} n/cm^2-s. All the dimensionless numbers are matched except the heat source number, which will mainly affect the peak temperature of the core structure.

Table 5 Scaling results of DHX and NDHX

Fluence ($\times 10^{25}$ n/m^2)		0	**0.1**	0.2	0.5	1	3-8
DHX Shell side	δ ratio	1.24	**1.35**	1.46	1.81	2.13	2.22
	D_h ratio	1.09	**1.19**	1.29	1.60	1.87	1.96
	h ratio	0.80	**0.73**	0.68	0.55	0.46	0.44
DHX Tube side	δ ratio	1.24	**1.35**	1.46	1.81	2.13	2.22
	D_h ratio	0.88	**0.96**	1.04	1.29	1.52	1.59
	h ratio	0.80	**0.73**	0.68	0.55	0.46	0.44
NDHX	δ ratio	1.24	**1.35**	1.46	1.81	2.13	2.22
	D_h ratio	0.88	**0.96**	1.04	1.29	1.52	1.59
	h ratio	0.80	**0.73**	0.68	0.55	0.46	0.44

SUMMARY

In the present work, by applying the scaling methodology developed in Ref. [1], the scaling results for a scaled-down experimental facility from a prototypic DRACS design were obtained. All the dimensionless numbers are matched except the heat source number, which will distort the peak temperature in the core during the transient.

REFERENCES

1. X. WANG, Q. LV, X. SUN, R.N. CHRISTENSEN, T.E. BLUE, G. YODER, D. WILSON, and P. SABHARWALL, "Scaling Analysis for the Direct Reactor Auxiliary Cooling System for AHTRs", submitted to American Nuclear Society 2011 Winter Meeting, October 30-November 3, Washington, DC (2011).
2. A.J. KARABELAS, T.H. WEGNER, and T.J. HANRATTY, "Use of Asymptotic Relations to Correlate Mass Transfer Data in Packed Beds", *Chemical Engineering Science*, **26**, 1581-1589 (1971).
3. P.F. PETERSON, "Modular Pebble-Bed AHTR Design Review", University of California, Berkeley, Design Status Update, October 7 (2009).

4. A. GRIVEAU, "Modeling and Transient Analysis for the Pebble Bed Advanced High Temperature Reactor (PB-AHTR)", UCBTH-07-001, University of California at Berkeley, Berkeley, CA (2007).
5. H. GOUGAR et al., "Prismatic Coupled Neutronics/Thermal Fluids Transient Benchmark of the MHTGR-350 MW Core Design", accessed from INL published material website (2010).
6. K.S. REDDY, and P.K. KARTHIKEYAN, "Combinatory Models for Predicting the Effective Thermal Conductivity of Frozen and Unfrozen Food Materials", *Advances in Mechanical Engineering*, Article ID 901376 (2010).
7. A.K. MOHANTY, and K.M. SAHOO, "Laminar Convection in Wall Sub-Channel and Transport Rates for Finite Rod-Bundle Assemblies by Superposition", *Nuclear Engineering and Design*, **92**, 169-180 (1986).
8. K.M. SAHOO, and A.K. MOHANTY, "Finite Element Analysis for Laminar Flow and Heat Transfer in Finite Rod Bundles", *Chem. Eng. Comm.*, **51**, 129-140 (1987).